Front. Biol. 2017, 12(3): 199–209
DOI 10.1007/s11515-017-1449-z

RESEARCH ARTICLE

Analysis of curcumin interaction with human serum albumin using spectroscopic studies with molecular simulation

Turban Kar[1], Pijush Basak[2], Srikanta Sen[3], Rittik Kumar Ghosh[1], Maitree Bhattacharyya (✉)[1,2]

[1] *Department of Biochemistry, University of Calcutta, 35, Ballygunge Circular Road, Kolkata-700019, West Bengal, India*
[2] *Jagadis Bose National Science Talent Search, Kolkata-700107, India*
[3] *229A/230, Mira Tower, Lake Town, Block-A, Kolkata-700089, India*

BACKGROUND: Curcumin has emerged to be utilized as a superb beneficial agent, due to its naturally occurring anti-oxidant, anti-inflammatory and anti-carcinogenic property.
METHODS: The interaction of curcumin with human serum albumin, the main *in vivo* transporter of exogenous substances, was investigated using absorption spectroscopy, steady-state fluorescence, excited state life-time studies and circular dichroism spectroscopy.
RESULTS: Isothermal titration calorimetry techniques inferred one class of binding site with binding constant $\sim 1.74 \times 10^5\ M^{-1}$ revealing a strong interaction. The binding profile was analyzed through the evaluation of the thermodynamic parameters, which indicated the involvement of hydrophobic interactions (burial of non-polar group). Fluorescence lifetime of tryptophan residue was observed to decrease to 1.94 ns from 2.84 ns in presence of Curcumin. Percentage of α helicity of human serum albumin was also reduced significantly upon binding with curcumin as evidenced by circular dichroism measurement leading to conformational modification of the protein molecule.
CONCLUSIONS: On the basis of such complementary results, it may be concluded that curcumin shows strong binding affinity for human serum albumin, probably at the hydrophobic cavities of the protein and at or around the tryptophan residue. Molecular Docking analysis of HSA and curcumin provided light on the number of binding sites at an atomic level, which were already determined at a molecular level in spectroscopic measurements. Our study unfolds the modes of interaction of curcumin with human serum albumin in the light of different biophysical techniques and molecular modeling analysis.

Keywords curcumin, human serum albumin, fluorescence quenching, conformational change, thermodynamic parameters

Introduction

Curcumin, the bioactive compound with certain drug based potential candidate has poor bioavailability and half-life. Most of the hydrophobic and acidic drugs get transported through the body by binding with Human Serum Albumin (HSA), this increases their half-life as well as they get circulated in the system. This polyphenolic compound may be isolated from Turmeric (*Curcuma long* L.) belonging to Zingiberaceae family. Curcumin has attracted considerable interest in recent times due to its wide spectrum activities in the realm of biological and pharmacological researches (Dickinson et al., 2004; Aggarwal et al., 2016). There is an increasing demand in the biomedical field for the identification of effective natural antioxidants which are inexpensive and easily available (Semiz et al., 2016), especially to avoid toxic side effects from new generation antibiotics and curcumin may be an ideal probe in this field of research (Stocker, 2016; Mothi et al., 2015). Many Indian medicinal plants, herbs, spices are considered to be potential sources of antioxidant compounds and in some cases; their active constituents have been characterized (Leung and Kee, 2009). Antioxidant compounds isolated, purified and characterized from dietary components, such as turmeric (*Curcuma longa*), Curry leaves (*Murrayakoeneigii*), Sundakai (*Solanumtorvum*), and Methi leaves (*Trigonella foenumgraecum*) effectively inhibit reactive oxygen species (ROS) induced lipid peroxidation and DNA damage (Lee et al., 2016).

Curcumin [1, 7-bis (4-hydroxy-3-methoxyphenyl)-1, 6-heptadiene-3, 5-Dione], a member of the curcuminoid family of compounds, is a yellow-orange pigment derived from the

Received December 7, 2016; accepted March 15, 2017
Correspondence: Maitree Bhattacharyya
E-mail: bmaitree@gmail.com

rhizome of Curcuma longa (Mazaheri et al., 2015; Maciazek-Jurczyk et al., 2013). Human serum albumin is the most abundant carrier protein and accounts for over 50% of the total plasma protein content, remaining at a concentration of almost 0.6 mM. Its properties span from ligand binding/transport functions to enzymatic and antioxidant activities. The X-ray crystal structure of Human Serum Albumin reveals three homologous domains assembled into a heart-shaped globular molecule, with each domain composed of two sub domains. Most of the backbone is α-helical, with the remaining polypeptide occurring in turns and extended or flexible regions connecting the domains (Aggarwal et al., 2003). The most outstanding property of serum albumin is its ability to bind a variety of endogenous and exogenous ligands, and crucial role on drug delivery (Salzano et al., 2011). The locations of various ligand binding sites have been found to be associated to some domain or sub domain in the past (Sudlow et al., 1975). In the light of such domain specific binding, these types of studies become interesting probes to monitor alterations of the topology of HSA during unfolding (Siddiqi et al., 2016).

In this study, binding of curcumin to serum albumin has been extensively investigated because of its pharmacokinetic and pharmacological significance. Spectroscopic techniques were utilized to analyze the binding parameters of curcumin to human serum albumin. Steady-state as well as lifetime decay was used to analyze the nature and modes of the interaction. CD spectroscopy was applied to investigate the conformational changes involved in this interaction. Binding and thermodynamic profile of the interaction was analyzed by exploiting Isothermal Calorimetry. Docking and molecular modeling was also employed to understand the mechanism of binding process. As IDB (Iodipamide) and curcumin (both keto and enol forms) are very similar in overall structure and the functional groups present we expected that the IDB binding site on HSA may be a potential binding site for curcumin. The present modeling work only demonstrated that the IDB binding site of HSA is really a potential binding site of curcumin on HSA. The binding modes have been characterized and the binding affinities have been estimated and compared with experimental data.

Materials and methods

Materials and sample preparation

Human Serum Albumin (HSA) and curcumin (99% pure) were purchased from Sigma Pvt. Ltd, USA and Hi-Media (India) respectively. Human serum albumin and curcumin solutions were prepared in milli-Q water maintaining weight/volume (w/v) ratio and fresh solutions were prepared before each experiment. All the experiments were performed in triplicate sets with three different concentrations for each.

Steady state fluorescence spectroscopy

All steady-state fluorescence measurements were performed in Varian carry eclipse spectrofluorometer, Human Serum Albumin (15 μM) was titrated with varying concentrations of curcumin (from 0 to 6.5×10^{-4} M) at 22°C. Samples were excited at 295 nm, and the fluorescence emission spectrum was scanned in the range of 310 to 510 nm with excitation and emission slits fixed at 2 nm. The quenching mechanism was interpreted by analyzing the Stern–Volmer plot and modified Stern–Volmer plot applying the formula: $F_0/F = 1 + K_{sv}$ [Q], Where F_0 and F are the steady-state fluorescence intensities in absence and presence of quencher respectively, [Q] is the concentration of the quencher, and K_{sv} is the Stern Volmer quenching constant, measuring the efficiency of quenching. The Stern–Volmer plot was analyzed to obtain various binding parameters for the interaction and the plot of F_0/F versus [Q] indicates a straight line and K_{sv} was worked out from the slope. The modified SV equation log $[(F_0 - F)/F)]$ = logK_a + n log [Q], (Lehrer, 1971) equation describes, the fraction of fluorescence quenched upon full ligation compared to the integrated protein. The binding constant (K_a) and the number of binding sites (n) calculated using the same equation (Basak et al., 2016). A plot of log $[(F_0–F)/F]$ vs. log [Q] gave a straight line whose slope is equal to n (binding sites) and the intercept on Y-axis to log K_a (K_a equal to the binding constant). Free energy of the reaction was calculated by using the following equation: $\Delta G = -RT\ln K_a = RT\ln K_d$, (Arias-Moreno et al., 2011), where ΔG is the Gibbs energy of binding, K_a is the association equilibrium constant, and K_d is the dissociation equilibrium constant.

Time-resolved fluorescence life time spectroscopy

Time resolved fluorescence study analyses the emission decay of the fluorescent probes providing an opportunity for multiplexed analysis of protein conjugates. The fluorescence lifetime can be sensitive to a great variety of internal factors defined by the fluorophore structure and external factors that include temperature, polarity, and the presence of fluorescence quenchers. A combination of environmental sensitivity and parametric independence mentioned above renders fluorescence lifetime as a separate yet complementary method to traditional fluorescence intensity measurements (Basak et al., 2016).

In our study fluorescence lifetime measurements were performed using HORIBA Jobin Yvon IBH product scientific time-correlated single photon counting (TCSPC). The samples were excited at 295 nm using a Nano LED pulsed laser. The instrument response function (IRF) was obtained using Ludox™ suspension. The full width at half maxima (FWHM) of the IRF was 877 ps. The emission decay data at 330 nm were analyzed using the software, DAS6, provided with the instrument.

Isothermal titration calorimetric measurements

Isothermal titration calorimetry (ITC) directly characterizes the thermodynamics of binding interactions and being a quantitative technique it determines the binding affinity (K_a), enthalpy changes (ΔH), and binding stoichiometry (n). Based on these initial measurements Gibbs energy changes (ΔG), and entropy changes (ΔS), was determined using the relationship:

$$\Delta G = -RT\ln K_a = \Delta H - T\Delta S.$$

The energetics of the binding of curcumin to Human Serum Albumin was studied using a VM2: Cell- ITC 200 (micro cal) titration micro calorimeter. The sample and reference cell of the calorimeter were loaded with protein solution each of 300 μL (3 mM) in aqueous solution. The protein and ligand concentration were fixed at 16 μM and 9 mM respectively. Then multiple injections of 80 μL of curcumin were made into the sample cell containing protein solution till saturation was reached for each protein separately. The basic method of ITC implies ligand concentration be kept 30 – 40 times more than protein concentration and a significant concentration to be maintained for the protein (Zaidi et al., 2013; Basak et al., 2015). Heats of dilution for the ligands were determined in control experiments and these were subtracted from the integrated data before curve fitting was performed using Origin Pro 9.0 (Northampton, USA).

Circular dichroism spectroscopy

The alteration in the secondary structure of the protein HSA in presence of curcumin was studied using JASCO-715 CD spectropolarimeter. Far-UV CD spectra of protein samples (1.0 μM) were recorded in presence of increasing concentration of curcumin till saturation was reached with a scan speed of 20 nm/min and a response time of 2 s. Each spectrum was baseline corrected and respective blanks were subtracted. Final plot was taken as an average of three accumulated plots in the range of 190–250 nm and molar ellipticity was calculated from the observed ellipticity (Baskaran et al., 2010).

Molecular modeling and binding profile

Spectroscopic study discussed so far provided detailed information regarding binding parameters and nature. However, spectroscopic studies in general cannot provide information of the binding at the atomic level; for example, it cannot provide direct evidence on the actual binding site as well as the binding mode of the small molecule to the protein, which is only possible by molecular modeling. Thus, spectroscopic studies and molecular modeling studies generally provide complementary information which provides a much complete understanding about the interactions. In the present case also we have analyzed through spectroscopic studies followed by docking based molecular modeling as discussed below.

Choice of the PDB file for docking

There are a number of co-crystal structures available in the protein database that can be used for various docking studies. However, it is important to choose the right kind of PDB file for making the docking study realistic. In our study, we have chosen the Human Serum Albumin co-crystal structure with PDB id 2BXN. IDB (Iodipamide) is the bound ligand in 2BXN. Comparison of the overall structural aspects like atomic group compositions, and size and shape with the two variants of curcumin indicates that these molecules are similar in these aspects. Thus the Iodipamide binding site on human serum albumin in this crystal structure is a potent site for the binding of curcumin. So we use the iodipamide binding site in the crystal structure 2BXN for performing the docking exercises for the two variants, the keto and enol forms of curcumin.

Generation of the 3D model of human serum albumin

We constructed a 3D model of the Human Serum Albumin using molecular modeling methods considering the co-crystal structure with PDB id 2BXN (Fig. 1). First of all we added H-atoms to the HSA part of the crystal structure 2BXN. The structure thus generated was then refined by minimizing the potential energy of the HSA part of the crystal structure using the ABNR algorithm in the molecular modeling software CHARMM 26b (Harvard University, Massachusetts) (Brooks et al., 1983).This allows rearrangement of the backbone and the side-chains to remove any distortion present into the crystal structure. For the electrostatic interaction a distance cutoff of 10Å was used. Energy minimization was performed for 1000 ABNR steps keeping the entire structure free. This 3D structure was used to perform the docking evaluations of the models of the keto and enol forms of the compound curcumin to the generated 3D model of HSA using the tool Autodock 4.0 (Scripps Research Institute, California). In the docking process we have considered the HSA structure as a rigid body.

Generation of the 3D models of the keto and enol forms of curcumin

The 3D structures of these compounds were generated and energy minimized by the Accelrys DS Visualizer 2.0 (BIOVIA, San Diego) and saved as PDB file. We have used these 3D models for docking based binding studies using Autodock 4.0 (Scripps Research Institute, California) (Masone and Chanforan, 2015; Biovia, 2016).

Setup and docking procedure

We followed the standard protocol of docking by Autodock 4.0. The Autodock program uses a rapid energy evaluation through pre-calculated grids of affinity potentials and a

variety of search algorithms to find suitable binding poses of the docked compound onto the target macromolecule (Prasad et al., 2013). The affinity and electrostatic maps were computed using a cubic grid of dimension 50Å × 50Å × 50Å with the grid points along the *x*, *y* and *z* axes and a grid spacing of 0.375 Å was used. The center of the grid was set at a position such that it covers well the IDB binding site of the model Human Serum Albumin. All the other parameters used were set to their default values. The Lamarckian genetic algorithm was used for the search and the results were analyzed based on binding energy. For each ligand, a docking experiment consisting of 20 simulations was performed. The poses of the docked compound were then ranked in order of increasing docking energies. The binding mode corresponding to the most favorable predicted binding energy was considered as the predicted binding mode of the compound.

Results

Fluorescence quenching of HSA in presence of curcumin

The fluoresence intensity decreases on the successive addition of curcumin and reaches to the saturation. The intensity variation behavior can be attributed to the relative exposure of the fluorophores on the addition of curcumin and the wavelength of the emission maximum is dependent on the microenvironment of the fluorophores which in present case is shifted toward the more hydrophobic environment as indicated by the prominent blue shift. The fluorescence spectrum of human serum albumin has a strong emission band (λ_{max}) at 338 nm due to the intrinsic tryptophan residues. Change of emission wavelength and decreased fluorescence intensity in presence of curcumin was observed in Fig. 1. There was a shift of 5 nm from the native state.

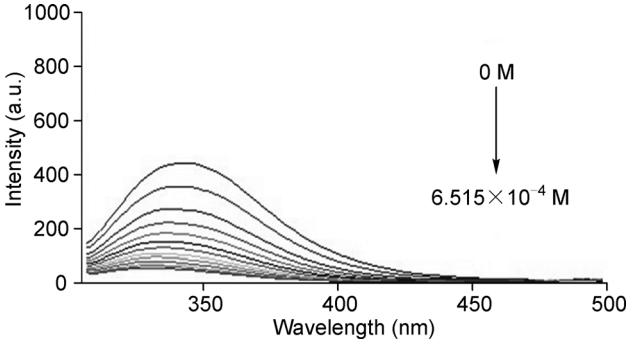

Figure 1 Fluorescence spectra of human serum albumin (15 μM) in presence of increasing amounts of curcumin; concentration corresponds from 0 μM to 650 μM. Axis acronyms – *X* axis (a.u. – arbitrary units); *Y* axis (nm – nanometers).

Fluorescence quenching might have generated by the formation of complexes at ground or excited state. The possible quenching mechanism was analyzed during the Stern–Volmer plot for curcumin–HSA systems shown in Fig. 2. The plot was observed to be nonlinear for both systems with increasing slopes; different parameters have been presented in Table 1.

When small molecules bind independently to a set of equivalent sites of a macromolecule, the equilibrium between free and bound molecules is represented by the equation:

$$\log(F_0 - F)/F = \log K + n\log[\mathrm{Q}]$$

where F_0 and F are the steady-state fluorescence intensities in absence and presence of quencher respectively, [Q] is the concentration of the quencher, K and n are the binding constant and number of binding sites, respectively. The values of K and n for Curcumin–HSA system were calculated from the intercept and slope of the plot of log $(F_0 - F)/F$ vs. log [Q] (Fig. 2). K_{sv} was obtained using the initial linear part of the quenching curve for lower quencher concentration (Airinei et al., 2011). The value of K is significant to understand the distribution of the drug in plasma since the weak binding can lead to a short lifetime or poor distribution, while strong binding can decrease the concentrations of free drug in plasma. The values of K and n are summarized in Table 1.

Decreased life-time of human serum albumin in presence of curcumin

Fluorescence lifetime serves as a sensitive parameter for exploring the interaction and the decay profile of the fluorophore. It is sensitive to excited state interaction, and for the emission from the residue three life-times were noted. The presence of three fluorescence life-times depends on the environment around the tryptophan residue and on the modes of interaction between the tryptophan residue and its microenvironment. We estimated lifetime decay of tryptophan residue in two protein states – native and conjugated with curcumin. The variation of the fluorescence life-times of tryptophan residues depend on its position within the protein primary structure.

Fluorescence lifetime decay profiles of the native human serum albumin and the curcumin protein complex have been presented in Fig. 3. Human serum albumin has only one tryptophan residue and the fluorescence lifetime of tryptophan residue in HSA was found to decrease significantly in presence of curcumin. Average excited state life time of tryptophan residue in HSA was observed to be significantly decreased from 2.84 ns to 1.93 ns during the interaction with curcumin (Table 2) which confirms the involvement of dynamic quenching. We fitted the decay profiles of human serum albumin bound to curcumin to triple exponential function to carry out time resolved fluorescence study to explore the nature of binding interactions of curcumin with human serum albumin. There were three lifetime components in native protein τ_1, τ_2 and τ_3, which contribute depending on the proteins multiple local configurations and changes in the extent of solvent accessibility.

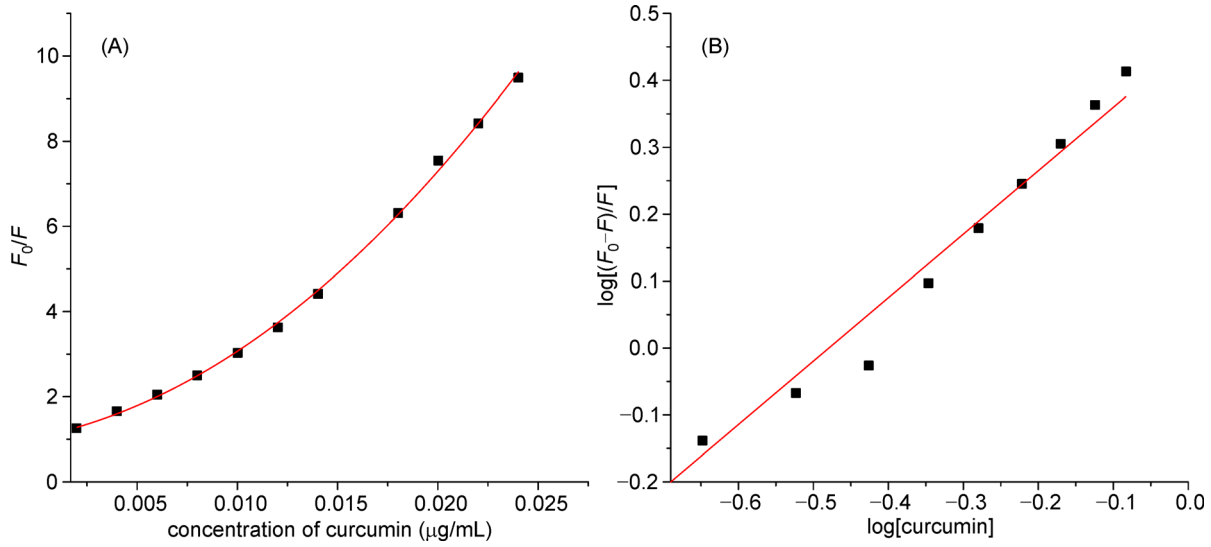

Figure 2 Panel (A) and (B) represent Stern–Volmer and modified Stern–Volmer plots of F_0/F and log $[(F_0-F)/F]$ vs. concentration of curcumin where the concentration of human serum albumin remains fixed at 15 μM.

Table 1 Quenching constant and curcumin binding parameters to HSA

Protein	Ligand	SV equation	R^2	K_{sv} ($10^3 mol^{-1}$)	Modified SV log $[(F_0-F)/F)]$ = logK_a + n log [Q]	R^2	Binding constant $K_a(10^3 mol^{-1})$	No. of binding site
Human serum albumin	Curcumin	$y = 375.36x - 0.3012$	0.9554	0.35	$y = 1.4024x + 3.1522$	0.992	1.419	1.402

Table 2 Fluorescence life time decay profile of Tryptophan in human serum albumin in absence and presence of curcumin

Protein		τ_1	τ_2	τ_3	Average (τ)	χ^2
Human serum albumin	Native	0.30	1.37	6.85	2.84	1.21
	Curcumin-HSA complex	0.80	1.67	3.34	1.93	1.40

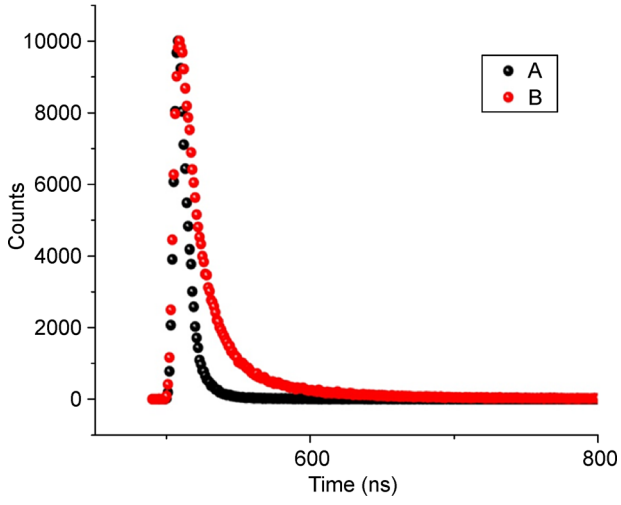

Figure 3 The fluorescence lifetime decay profiles of the (A) protein-curcumin complex and (B) native HSA; Axis acronyms – *X* axis (ns – nanoseconds).

Involvement of hydrophobic forces in human serum albumin-curcumin interaction

The thermodynamic aspect of binding of ligand with macromolecule is best understood by ITC and is characterized by the stoichiometry (n), the association constant (K_a), the change in free energy (ΔG), enthalpy (ΔH), entropy (ΔS), and heat capacity of binding (ΔCp). ITC measures the binding equilibrium directly by determining the heat evolved on association of a ligand with its binding partner. We explored the energetics of binding of curcumin with HSA protein utilizing ITC.

ITC provides a direct method to determine thermodynamic characterization of non-covalent, equilibrium interactions involving small molecules with protein macromolecule (Forli et al., 2016). A representative calorimetric titration profile of human serum albumin has been provided in Fig. 4 which presents data for the titration of human serum albumin (15μM) with curcumin at pH 7.0 and 298 K, showing calorimetric response as successive injections were added to

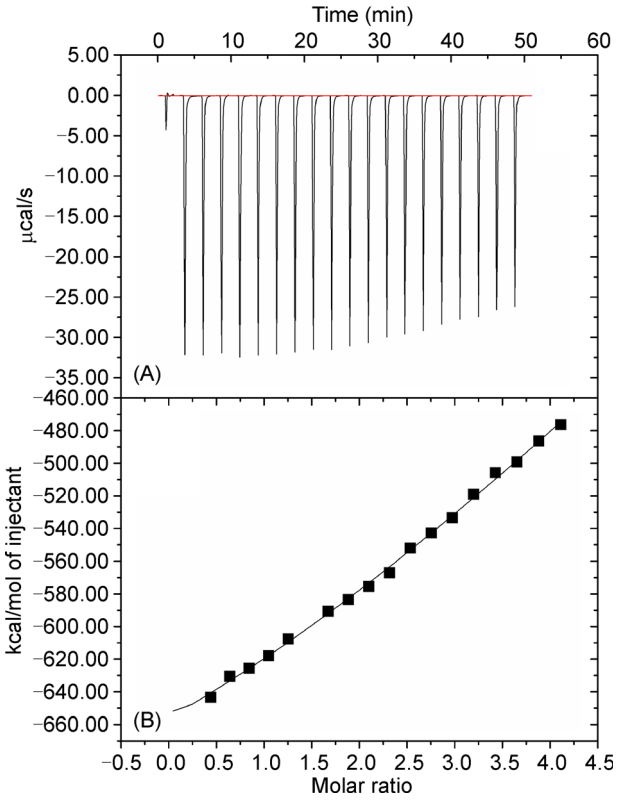

Figure 4 Isothermal titration calorimetric profiles for the binding of curcumin to Human serum albumin. The top panel (A) represents raw data for the sequential injection of curcumin solution (80 µM) into HSA (3 µM) solution. The lower panels (B) show the integrated heat results after correction of heat of dilution against the mole ratio of Human serum albumin /curcumin. The points (closed squares) were fitted to a one-site model and the solid lines represent the best-fit results.

the sample cell. A standard nonlinear least squares regression binding model involving one binding site fitted well to the data. The solid line shown in Fig. 4 (panel B) is the best fit to the experimental values. Thermodynamic data associated with the binding of curcumin and Human Serum Albumin has been summarized in Table 3. Each value in this table is an average of three independent experiments.

Analysis of thermodynamic data indicates that Human Serum Albumin interacts with curcumin exothermally and both entropy and enthalpy driven (Table 3). Interestingly, large negative free energy $\Delta G° = -6.06$ kcal/mol and enthalpy value $\Delta H° = -37.55 \times 10^6$ kcal/mol value indicate that the binding is favorable. The binding stoichiometry for curcumin and human serum albumin was around 1.1. This clearly showed that curcumin binding to human serum albumin is largely contributed by negative entropy $\Delta S = -12.68 \times 10^6$ kcal/mol.

Altered secondary structure of HSA in presence of curcumin

Circular dichroism (CD) is one of the strong and sensitive spectroscopic techniques to explore various aspects of protein structure and to analyze its interaction with small molecules. Far-UV region (190–250 nm) is used to investigate secondary structure content of proteins as the main absorbing groups in this region are peptide bonds. Because of the asymmetric protein environment and consequently its inherent chirality, the induced asymmetry of some achiral ligand molecules is observed during the irreversible binding interaction. CD spectroscopy can monitor induced optical activity in the visible as well as UV range of light absorption.

Circular dichroism was performed to monitor if any secondary structural alterations is involved. The results have been expressed as MRE (mean residue ellipticity) in deg cm^2/dmol, which is given by

$$\mathrm{MRE(mdeg)} = \theta_{\mathrm{obs}}/(10\ n \cdot c \cdot l)$$

where, θ_{obs} is the observed ellipticity in millidegrees, c is the concentration of protein in mol/L, l is the length of the light path in centimeters and n is the number of peptide bonds.

CD data may be analyzed by the following formula:

$$\%\alpha - \mathrm{helix} = [(\mathrm{MRE}_{222\mathrm{nm}} - 2340)/30300] \times 100$$

The CD spectra were recorded in the wavelength range of 190–300 nm to study the influence of curcumin on the secondary structure of Human Serum Albumin where standard negative bands at 208 and 220 nm (Fig. 5) characterizes the asymmetric environment of aromatic chromophores and typical α-helical structure (Pattanayak et al., 2016). The α-helicity content of Human Serum Albumin in absence and presence of different concentrations of curcumin have been listed in Table 4.

Molecular modeling of curcumin binding to human serum albumin

Comparison of the binding constants and the binding modes of the docked compounds

With the default setting Autodock predicts the binding energy of a compound and its binding constant (K_i) for ten separate docking trials. The best estimated binding energies and the binding constants (K_i) values for each of the three docked

Table 3 Thermodynamic parameters for HSA-Curcumin interaction derived by ITC method

Protein	Ligand	Binding constant ($10^3 mol^{-1}$)	Enthalpy change (kcal/mol)	Entropy change (kcal/mol)	Free energy change (ΔG) (kcal/mol)	Process
Human serum albumin	Curcumin	1.11	-37.55×10^6	-12.68×10^6	−6.06	van Der Waal's interaction and hydrogen bonding

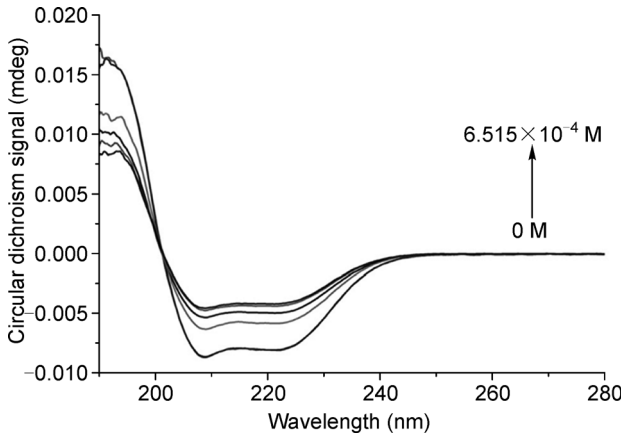

Figure 5 Circular dichroism spectra of HSA observed at 25°C in presence of increasing concentration of curcumin (0 μM to 650 μM). Axis acronyms – *X* axis (nm – nanometers); *Y* axis (mdeg – millidegrees).

Table 4 Estimation of secondary structure content of human serum albumin with gradually varying concentration of curcumin

Concentration of curcumin (M)	α-helix (%)
0	51
4.343×10^{-4}	47.6
4.886×10^{-4}	47.4
5.429×10^{-4}	46.5
5.972×10^{-4}	45.3
6.515×10^{-4}	43.3

compounds are summarized in Table 5. It may be pointed out here that in solution curcumin exists as a mixture of keto form and enol form of curcumin and it is practically not possible to isolate them. Thus, it is not possible to measure experimentally the binding energies of keto form and enol form of Curcumin separately. On the other hand, molecular modeling has the opportunity to treat them separately and hence can provide their binding energies and binding constants separately. It is interesting to note that the binding energies of the two forms as estimated by docking are significantly different, the keto form being more potent than the enol form.

The docked structures of the keto form and the enol form with the full structure of Human Serum Albumin are shown in Fig. 6. The binding energy of the best (lowest energy) docked poses and the binding constant estimated is summarized in Table 5, the values have been obtained using Molecular Docking platform (Autodock 4.0). The docked structures representing the binding modes of the two variants (keto and enol) of Curcumin with the protein neighborhood are shown in Fig. 7. The curcumin variants are shown as ball and stick models. The protein neighborhood is represented in wire-frame style. It indicates that there is strong interaction between the carbonyl oxygen atoms in keto-curcumin and the residue Lys-199. Some interaction is also seen between the

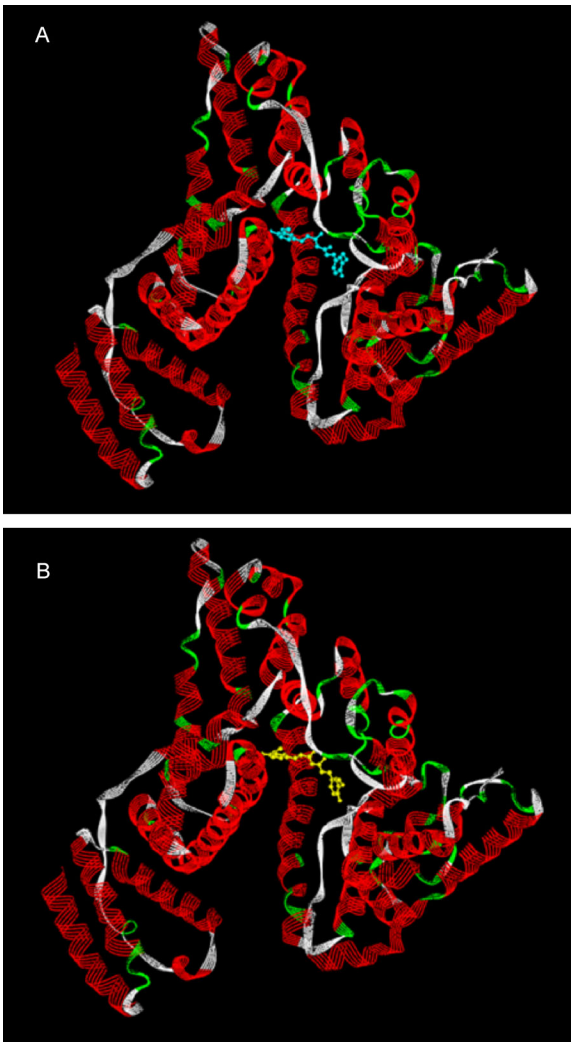

Figure 6 The docked structures of (A) the keto form and (B) the enol form are shown. The keto-curcumin is shown in cyan ball and stick model and the enol-curcumin is shown in yellow ball and stick model. The Human serum albumin structure is represented in line-ribbon style.

residue His-168 and the carbonyl oxygen and the hydroxyl oxygen of one terminal ring of curcumin (Fig. 7A). Very similar interaction mode is found for the enol-form of curcumin as shown in (Fig. 7B). Comparison of the binding modes of the two forms of curcumin is shown in (Fig. 8). The keto-form is represented as ball and stick while the enol-form is shown in stick model. The binding modes are found to be very similar even though slight differences in the positions of the interacting atoms of curcumin may cause a difference in binding constant as evident from Table 5.

To assess the solvophobic effect on the ligand binding we have compared the SASA (solvent accessible surface area) between the HSA in complex generated by docking method and free form and obtained how much SASA has been protected from the solvent by the bound ligand. In a similar way we have estimated the SASA of curcumin has been

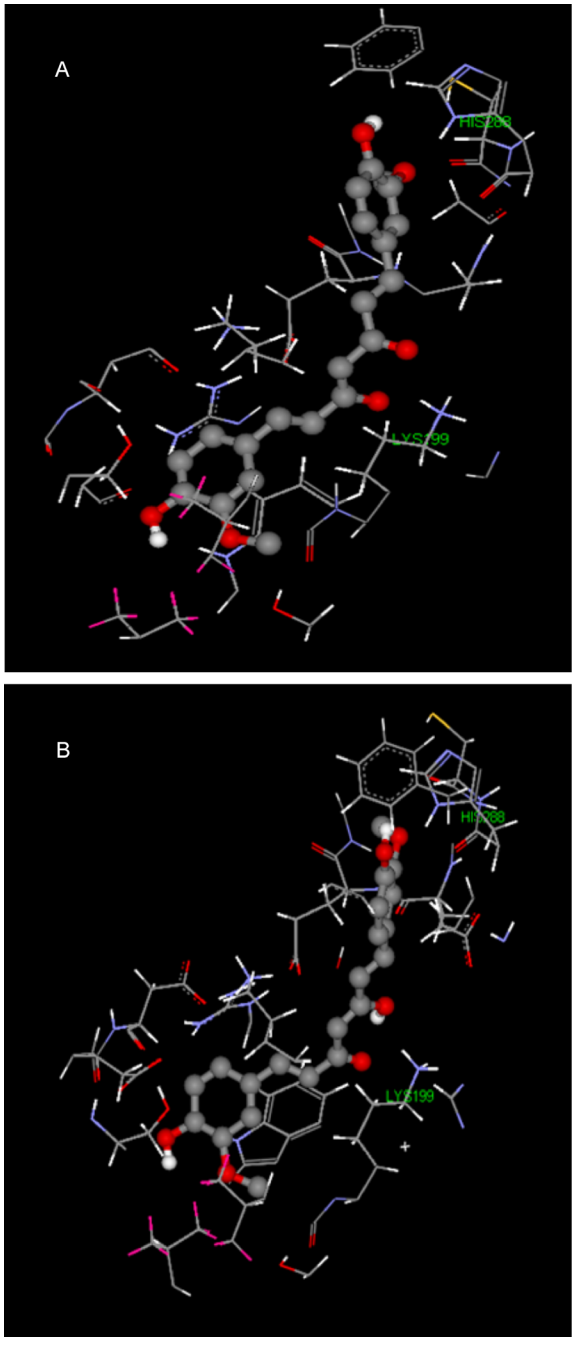

Figure 7 The docked structures of (A) the keto form and (B) the enol form with its protein neighborhood are shown. The curcumin variants are shown as ball and stick model. The Human serum albumin neighborhood is represented in wireframe style.

protected from the solvent by HSA in the docked complex. We have used the tool MOLMOL for computing the SASA of a molecule in its free form and complex form. We have further estimated the effect of change in SASA due to complex formation, by using the method of Eisenberg (Singh et al., 2014). In Eisenberg's method the change in free energy due to change in SASA value is given by $\Delta G = \sum_{i=1}^{n} \Delta A_i \sigma_i$ where

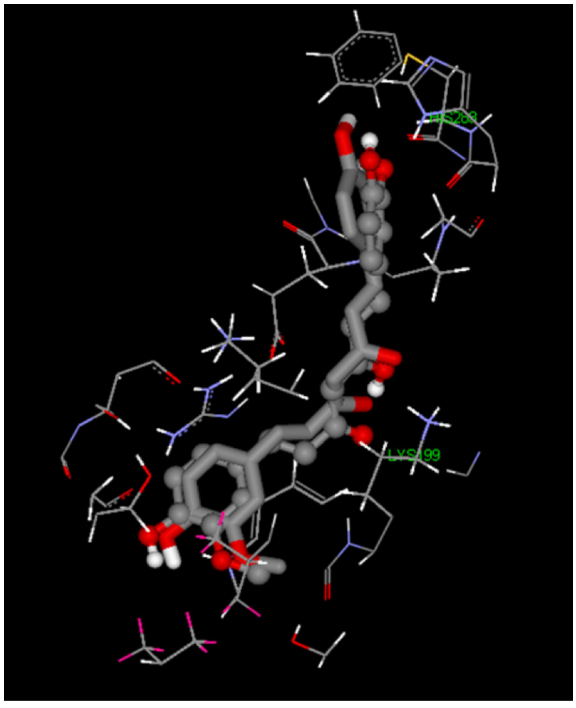

Figure 8 Comparison of the binding modes of the two forms of curcumin. The keto-form is represented as ball and stick while the enol-form as shown in stick form.

Table 5 The best binding energies and the computed binding constants obtained by the docking runs for two different forms of curcumin. The values have been obtained using molecular docking platform (Autodock 4.0)

Molecule name	$\Delta G_{binding}$(kcal/mol)	K_i (μM)	K_i (μM) experimental
Curcumin (keto form)	−7.32	4.3	1.79
Curcumin (enol form)	−6.92	8.4	

ΔA_i is the change in SASA of the i^{th} atom of the protein and σ_i is the atomic salvation parameter of the i^{th} atom (Hou et al., 2005). σ_i depends on the type of the i^{th} atom (Hou et al., 2005). MOLMOL also provides the SASA values at the atomic level. The results are summarized in Table 6. The results indicate that in forming each complex a significant contribution comes from the solvophobic effect.

Discussion

This study provides valuable information about interaction of curcumin, a bioactive plant-derived compound with the important carrier protein human serum albumin. Fluorescence quenching measurements (Fig. 2) revealed that the tryptophan residue of human serum albumin was placed in a more hydrophobic environment which may have originated due to

Table 6 Change in SASA values for HSA and curcumin molecule due to complex formation and the free energy change due to complex formation

		HSA-Curcumin (keto)		HSA-Curcumin (enol)	
		HSA	Curcumin	HAS	Curcumin
1	ΔSASA (Å^2)	−387.0	−539.4	−370.4	−539.4
2	ΔG (kcal/mol)	−2.33	−3.89	−2.26	−3.77

the changes in basic conformation of human serum albumin by making the structure more hydrophobic for tryptophan. The binding constant $K_{CUR–HSA} = 1.42 \times 10^3$ M^{-1} suggests high affinity binding of the curcumin to the carrier protein HSA. The number of binding site (n) indicates the location of the drug on HSA. The number of binding sites (n) for curcumin bound Human Serum Albumin was noticed to be 1.4 (rounded to nearest integer value 1) indicating that there was one independent class of binding site to be available on the protein for curcumin. Fluorescence excited state lifetime of tryptophan residue in HSA was found to decrease significantly from 2.84 ns to 1.93 ns during the interaction with curcumin (Table 2) confirming the involvement of dynamic quenching. There is only one Tryptophan residue present in HSA at position 214 (Sahoo et al., 2009). Therefore, the quenching of Human Serum Albumin fluorescence by curcumin may have originated from the interaction of Trp-214 and its micro-environment, thus inducing a decrease in the fluorescence intensity. In lifetime study the behavior of the excited state was assumed to have no relation to the ground state mechanisms. Curcumin can access both hydrophobic and hydrophilic sites of a protein. Since, the lifetime is affected by the presence of quencher (Curcumin), it is a case of both static and dynamic quenching as represented in Fig. 2A, and thus K_{sv} is derived from initial linear part of the curve as well from the modified Stern–Volmer Plot. On the basis of such complementary result, it may be inferred that curcumin shows strong binding to HSA, probably at the hydrophobic cavities of the protein. Molecular modeling has explained the interaction on the basis of the important role of the hydroxyl phenolic group of curcumin in the binding process. Experiment established (Fig. 2) that dynamic quenching was involved in the binding process and this was again verified by time resolved life-time study (Fig. 3). Since the protein possesses only one tryptophan residue, that may be responsible for the fluorescence signals. Fluorescence life-time data indicates that tryptophan residue emits multiple life-times, in native as well as in complexed state confirming the presence of dynamic quenching. In general fluorescence life-time is dependent on the intrinsic properties of the tryptophan in the excited state. Thermodynamic parameters for human serum albumin and curcumin interaction were evaluated using isothermal titration calorimetry (itc), which is in good agreement to the previously estimated parameters (Zhang et al., 2012). The observed enthalpy change upon the binding of curcumin with HSA usually includes the contribution of dehydration entropy change from the release of structured water molecules surrounding curcumin and Human Serum Albumin, and a conformational alteration usually reflects various contributions of Vander Waals interaction, hydrogen bonding, and electrostatic interaction. On the other hand, the entropy changes upon binding of curcumin with HSA. Thus, the interpretation of the observed enthalpy and entropy changes may not be simple but include various other factors. We estimated the binding parameters utilizing spectrofluorometry and Isothermal Titration Calorimetric techniques since virtually all binding processes are accompanied with uptake or release of heat. Moreover, higher concentrations of probe are advantageous for analyzing macromolecule-ligand interactions. This allows us to examine binding of curcumin in more detail at an extended concentration range of curcumin. The binding affinity analyzed with fluorescence spectroscopy took into consideration the location of quencher and fluorophore and moreover measures local changes around the fluorophores associated with the optical transition. Hence to address all these shortcomings, we have also authenticated the parameters by ITC measurements which consider overall global changes in the solution. On titration with increasing concentration of curcuminin studying CD spectrum, the negative bands of human serum albumin decreased in intensity without any shifts at the maximum wavelength, indicating a gradual decrease in the helical content of Human Serum Albumin with consequent partial unfolding of the global tertiary structure (Fig. 4). α helicity content of human serum albumin was decreased from 51% to 43.3% with concomitant increase of the β sheet content and random coil when curcumin was added to native human serum albumin (15×10^{-6} M).Thus loss of helical stability and associated unfolding were observed in the protein when interacted with curcumin. Human serum albumin being transport protein, curcumin induced unfolding might have altered its transport properties which in turn may affect different biological processes in the system. Molecular modeling result shows there is strong interaction between the carbonyl oxygen atoms in keto-curcumin and the residue Lys-199. Some interaction was observed between the residue His-168 and the carbonyl oxygen and the hydroxyl oxygen of one terminal ring of curcumin. It is interesting to note that the binding energies of the two forms as estimated by docking are significantly different, the keto form being more potent than the enol form. On the basis of the available consistent results, it may be concluded that the binding of curcumin with Human Serum Albumin might affect the microenvironment of Trp-214 which was also associated with the conformational change of human serum albumin (Sahoo et al., 2009; Gupta et al., 2011; Cheng et al., 2013).

Acknowledgments

We acknowledge UGC-DAE for providing fellowship to Turban Kar. We are also grateful to DST (FIST), World Bank-ICZMP (54-ICZMP/3P),

UGC-CAS, UGC-UPE, and DBT-IPLS, Government of India for providing the instrumental facility in the Department of Biochemistry, Calcutta University.

Compliance with ethics guidelines

The authors completely acknowledge the above mentioned funding agencies for grants. The authors Turban Kar, Pijush Basak, Srikanta Sen, Rittik Kumar Ghosh and Maitree Bhattacharyya declare no conflicts of interest.

References

Aggarwal B B, Kumar A, Bharti A C (2003). Anticancer potential of curcumin: preclinical and clinical studies. Anticancer Res, 23(1A): 363–398

Aggarwal M L, Chacko K M, Kuruvilla B T (2016). Systematic and comprehensive investigation of the toxicity of curcuminoidessential oil complex: A bioavailable turmeric formulation. Mol Med Rep, 13 (1): 592–604

Airinei A, Tigoianu R I, Rusu E, Dorohoi D O (2011). Fluorescence quenching of anthracene by nitroaromatic compounds. Dig J Nanomater Biostruct, 6(3): 1265–1272

Basak P, Debnath T, Banerjee R, Bhattacharyya M (2016). Selective binding of divalent cations towardheme proteins. Front Biol, 11(1): 32–42

Basak P, Pattanayak R, Bhattacharyya M (2015). Transition metal induced conformational change of heme proteins. Spectrosc Lett, 48 (5): 324–330

Baskaran N, Manoharan S, Balakrishnan S, Pugalendhi P (2010). Chemopreventive potential of ferulic acid in 7,12-dimethylbenz[a] anthracene-induced mammary carcinogenesis in Sprague-Dawley rats. Eur J Pharmacol, 637(1-3): 22–29

Biovia D S (2016). Discovery Studio Modeling Environment, Release 2017.DassaultSystèmes, San Diego, CA

Brooks B R, Bruccoleri R E, Olafson B D, States D J, Swaminathan S, Karplus M (1983). CHARMM: a program for macromolecular energy, minimization, and dynamics calculations. J Comput Chem, 4 (2): 187–217

Cheng Z J, Zhao H M, Xu Q Y, Liu R (2013). Investigation of the interaction between indigotin and two serum albumins by spectroscopic approaches. JPA, 3(4): 257–269

Dickinson D A, Levonen A L, Moellering D R, Arnold E K, Zhang H, Darley-Usmar V M, Forman H J (2004). Human glutamate cysteine ligase gene regulation through the electrophile response element. Free Radic Biol Med, 37(8): 1152–1159

Forli S, Huey R, Pique M E, Sanner M F, Goodsell D S, Olson A J (2016). Computational protein-ligand docking and virtual drug screening with the AutoDock suite. Nat Protoc, 11(5): 905–919

Gupta S C, Prasad S, Kim J H, Patchva S, Webb L J, Priyadarsini I K, Aggarwal B B (2011). Multitargeting by curcumin as revealed by molecular interaction studies. Nat Prod Rep, 28(12): 1937–1955

Hou T, Zhang W, Huang Q, Xu X (2005). An extended aqueous solvation model based on atom-weighted solvent accessible surface areas: SAWSA v2.0 model. J Mol Model, 11(1): 26–40

Lee H Y, Kim S W, Lee G H, Choi M K, Jung H W, Kim Y J, Kwon H J, Chae H J (2016). Turmeric extract and its active compound, curcumin, protect against chronic CCl4-induced liver damage by enhancing antioxidation. BMC Complement Altern Med, 16(1): 316

Lehrer S S (1971). Solute perturbation of protein fluorescence. The quenching of the tryptophyl fluorescence of model compounds and of lysozyme by iodide ion. Biochemistry, 10(17): 3254–3263

Leung M H, Kee T W (2009). Effective stabilization of curcumin by association to plasma proteins: human serum albumin and fibrinogen. Langmuir, 25(10): 5773–5777

Maciążek-Jurczyk M, Maliszewska M, Pożycka J, Równicka-Zubik J, Góra A, Sułkowska A (2013). Tamoxifen and curcumin binding to serum albumin.Spectroscopic study. J Mol Struct, 1044: 194–200

Masone D, Chanforan C (2015). Study on the interaction of artificial and natural food colorants with human serum albumin: A computational point of view. Comput Biol Chem, 56: 152–158

Mazaheri M, Moosavi-Movahedi A A, Saboury A A, Rezaei M H, Shourian M, Farhadi M, Sheibani N (2015). Curcumin mitigates the fibrillation of human serum albumin and diminishes the formation of reactive oxygen species. Protein Pept Lett, 22(4): 348–353

Mothi N, Muthu S A, Kale A, Ahmad B (2015). Curcumin promotes fibril formation in F isomer of human serum albumin via amorphous aggregation. Biophys Chem, 207: 30–39

Pattanayak R, Basak P, Sen S, Bhattacharyya M (2016). Interaction of KRAS G-quadruplex with natural polyphenols: A spectroscopic analysis with molecular modeling. Int J Biol Macromol, 89: 228–237

Prasad P, Khan I, Kondaiah P, Chakravarty A R (2013). Mitochondria-targeting oxidovanadium(IV) complex as a near-IR light photocytotoxic agent. Chemistry, 19(51): 17445–17455

Sahoo B K, Ghosh K S, Dasgupta S (2009). Molecular interactions of isoxazolcurcumin with human serum albumin: spectroscopic and molecular modeling studies. Biopolymers, 91(2): 108–119

Salzano A M, Renzone G, Scaloni A, Torreggiani A, Ferreri C, Chatgilialoglu C (2011). Human serum albumin modifications associated with reductive radical stress. Mol Biosyst, 7(3): 889–898

Semiz G, Çelik G, Gönen E, Semiz A (2016). Essential oil composition, antioxidant activity and phenolic content of endemic Teucrium alyssifolium Staph. (Lamiaceae). Nat Prod Res, 30(19): 2225–2229

Siddiqi M K, Alam P, Chaturvedi S K, Khan R H (2016). Anti-amyloidogenic behavior and interaction of Diallylsulfide with Human Serum Albumin. Int J Biol Macromol, 92: 1220–1228

Siddiqi M K, Alam P, Chaturvedi S K, Khan R H (2016). Anti-amyloidogenic behavior and interaction of Diallylsulfide with Human Serum Albumin. Int J Biol Macromol, 92: 1220–1228

Singh D V, Bharti S K, Agarwal S, Roy R, Misra K (2014). Study of interaction of human serum albumin with curcumin by NMR and docking. J Mol Model, 20(8): 2365

Stocker R (2016). Antioxidant defenses in human blood plasma and extra-cellular fluids. Arch Biochem Biophys, 595: 136–139

Stocker R (2016). Antioxidant defenses in human blood plasma and extra-cellular fluids. Arch Biochem Biophys, 595: 136–139

Sudlow G, Birkett D J, Wade D N (1975). The characterization of two specific drug binding sites on human serum albumin. Mol Pharmacol, 11(6): 824–832

Zaidi N, Ajmal M R, Rabbani G, Ahmad E, Khan R H (2013). A comprehensive insight into binding of hippuric acid to human serum albumin: a study to uncover its impaired elimination through hemodialysis. PLoS One, 8(8): e71422

Zhang Y, Golub L M, Johnson F, Wishnia A (2012). pKa, zinc- and serum albumin-binding of curcumin and two novel biologically-active chemically-modified curcumins. Curr Med Chem, 19(25): 4367–4375